A VOLUME FORCING METHOD BASED ON A RECONSTRUCTION-LIKE PROCEDURE FOR HYBRID RANS/LES

Jérémie Janin
Institut de Radioprotection et de Sûreté Nucléaire (IRSN)
Saint Paul Lez Durance, 13115 France
Aix-Marseille Univ., CNRS,
Centrale Marseille, M2P2 Marseille, France
jeremie.janin@irsn.fr

Fabien Duval
Institut de Radioprotection et de Sûreté Nucléaire (IRSN)
Saint Paul Lez Durance, 13115 France

Christophe Friess
Aix-Marseille Univ., CNRS,
Centrale Marseille, M2P2 Marseille, France

Pierre Sagaut
Aix-Marseille Univ., CNRS,
Centrale Marseille, M2P2 Marseille, France

ABSTRACT

Hybrid RANS/LES methods usually require a forcing method to trigger turbulence in LES regions, especially when there is no hydrodynamic instabilities to generate turbulence. A forcing method is proposed based on a reconstruction approach which consists in enriching the resolved velocity signal in the momentum equations. Only the extra terms that are considered to be prevalent for the turbulent production are retained. The proposed approach is assessed on the configuration of the planar jet case.

INTRODUCTION

Explosion risks, especially those related to hydrogen releases, are encountered in a large number of situations. These include for instance hydrogen leaks from pipes or storages in ventilated rooms (Taveau (2011)) or, during a severe accident in nuclear reactor containment vessels, hydrogen production due to the oxidation of zirconium (Bentaib *et al.* (2015)). In evaluating explosion hazards, the first stage consists in predicting the release and the turbulent mixing of flammable species. The cost and reliability of numerical simulations depend on the approach adopted for the turbulence modeling. One usually distinguishes two modeling approaches: the Reynolds-Averaged Navier-Stokes (RANS) statistical approach, that consists in modeling all turbulent scales, and the Large Eddy Simulation (LES) approach that consists in a direct calculation of the large scales and a modeling of the small ones. The RANS approach has the advantage of presenting reasonable computational costs but the reliability of the simulations may depend strongly on the level of sophistication of the turbulence model. On the other hand, the LES approach is much more predictive but requires larger computing times that can be out of reach when simulating large facilities with long transients. In this frame, hybrid RANS/LES methods are a very attractive alternative but pose the difficulty of generating turbulent fluctuations in transition zones. In this work, this difficulty is adressed by means of a volume forcing method. Numerical calculations using the open-source software CALIF^{3}S-P^{2}REMICS (2021) are carried out on a planar turbulent jet at $Re = 10000$ to assess and illustrate the interest of the proposed approach.

Forcing methods consist usually in adding a body force to the Navier-Stokes equations. Most of the time, target statistical quantities such as mean velocity and turbulent kinetic energy need to be defined as inputs for the forcing term. These statistical quantities could come from either a precursor simulation as in Pamier *et al.* (2009) or from the RANS upstream domain as in de Laage de Meux *et al.* (2015). For the latter, the forcing is applied to a channel flow which has an homogeneous energy distribution in the streamwise direction. Therefore, the use of values from the RANS upstream domain as targets, appears relevant. In non-homogeneous flows, the turbulent kinetic energy can significantly vary in the streamwise direction. For this reason, we propose here another approach which consists of deriving the target quantities from a prescribed kinetic energy ratio between resolved and subgrid scales.

The forcing method is tested upon the planar jet test case for which there exists various Direct Numerical Simulation (DNS) data in the literature such as Stanley (2002), Klein (2003), Le Ribault *et al.* (1999) and Engelmann *et al.* (2021). Stanley (2002) and Le Ribault *et al.* (1999) performed respectively DNS and LES simulations at Reynolds number of 3000. Klein (2003) provided DNS results for Reynolds number in the range of 1000 to 6000 but only results at $Re = 4000$ are reported here. The simulations presented here are performed with Reynolds number $Re = 10000$ as in Engelmann *et al.* (2021). In the present work, the first step was to compare a computation with turbulent inlet boundary conditions and a computation with laminar inlet boundary condition in addition with the forcing method. For these two simulations, it was observed that the results were very similar. This is due to the location of the forcing area which is situated at the entrance of the domain, just after the laminar velocity inlet. In this case the forcing acts ultimately as a turbulent boundary condition. In order to move away from this configuration, we proposed here a configuration inspired by RANS/LES zonal methods by imposing the turbulent kinetic energy ratio on the first diameters of the jet to enforce a RANS zone, and then switching to a non-zonal hybrid method with a self-adaptive reconstruction method. We focus in this work on the capability of the method to reproduce the expected self-similar profiles downstream from the RANS domain. We focus further on the center-line resolved and subgrid scale turbulent kinetic energy profiles with respect to the prescribed kinetic energy ratio.

In the next section, the reconstruction approach is presented as well as the employed turbulent model. In addition, the synthetic velocity used in the reconstruction procedure is briefly recalled. Finally, the advantages and drawbacks of the method on the studied case of the planar jet are discussed.

METHODOLOGY

In this study we suggest to use a reconstruction-like procedure as in Janin *et al.* (2021) to trigger turbulence in transition zones. The reconstruction procedure consists in adding a fluctuating part, that corresponds here to a synthetic velocity, to the resolved velocity. This operation introduces additional terms into the filtered Navier-Stokes equations. Usually, only the unsteady term is retained (Schmidt & Breuer (2017)) requiring, at least formally, that turbulence is statistically homogeneous. However, the flow of interest involves shear flow turbulence and this calls to retain a convective term related to the reconstruction procedure. We follow the motivations of Lundgren (2003) regarding the physical meaning of his linear forcing and we also retain here the term proportional to the resolved velocity gradient. Similar developments have been followed using either an unsteady forcing term (Schmidt & Breuer (2017)) or a forcing term proportional to the velocity gradient (**?**,Zhang (2021)). Here, both contributions are retained with the proposed reconstruction approach and the resulting filtered Navier-Stokes equations read:

$$\frac{\partial \tilde{u}_i}{\partial t} + \tilde{u}_j \frac{\partial \tilde{u}_i}{\partial x_j} = -\frac{1}{\rho}\frac{\partial \tilde{p}}{\partial x_i} + \nu \frac{\partial^2 \tilde{u}_i}{\partial x_j \partial x_j} - \frac{\partial \tau_{ij}}{\partial x_j} - \frac{\partial u_i^s}{\partial t} - u_j^s \frac{\partial \tilde{u}_i}{\partial x_j}$$

In the above equation $\tilde{u}_i$, $\tilde{p}$, ν are respectively the resolved velocity, the resolved pressure, the kinematic viscosity and τ_{ij} refers to the subgrid stresses which are modeled here using the Boussinesq's closure in combination with a subgrid scale eddy viscosity. The subgrid scale eddy viscosity is estimated in the frame of the Equivalent-Detached-Eddy Simulation (E-DES) approach proposed by Friess *et al.* (2015) using a two-equation k_{sgs}-ε_{sgs} subgrid scale model. In this approach, the control of the energy partition between resolved and subgrid scales is performed in a similar way as in the usual DES method by introducing the following limiter that multiplies the dissipation term in the k_{sgs}-equation:

$$F_{E-DES} = max\left[1, \frac{k_{sgs}^{3/2}}{\varepsilon_{sgs} L_{E-DES}}\right] \tag{1}$$

The length scale L_{E-DES} is defined as a function of a target turbulent kinetic energy ratio (Friess *et al.*, 2015) as

$$L_{E-DES} = \frac{r_k^{3/2}}{1 + \frac{c_{\varepsilon_2} - c_{\varepsilon_1}}{c_{\varepsilon_1}}\left[1 - r_k^{c_{\varepsilon_1}/c_{\varepsilon_2}}\right]} \frac{k^{3/2}}{\varepsilon_{sgs}} \tag{2}$$

where $r_k = k_m/k$ is the energy ratio, k_m the turbulent kinetic energy related to the unresolved scales, and k the total turbulent kinetic energy.

Here, we take benefit of the prescribed kinetic energy ratio to drive the synthetic velocity as suggested in a previous work (Janin *et al.*, 2021). The synthetic velocity involved in the reconstruction approach is derived from the Random Fourier Modes (RFM) method developed by Kraichnan (1970), and extended later by Fung *et al.* (1992), which is briefly recalled below:

$$u_i^s(x_j, t) = 2\sum_{n=1}^{N} \hat{u}_n \cos(\kappa_l^n x_l + \psi_n + \omega_n t)\sigma_i^n \tag{3}$$

where $\hat{u}_n$, ψ_n, ω_n and σ_i^n correspond respectively to the amplitude, the phase, the time frequency and the direction of the n^{th} Fourier mode related to the wave vector κ_i^n. The amplitude is written as $\hat{u}_n = \sqrt{E(\kappa_n)\delta\kappa_n}$, in which $E(\kappa)$ is a prescribed energy spectrum. The stochastic frequency $\omega_n = \lambda U_{rms}\kappa_n$ corresponds to the sweeping hypothesis where λ follows a normal distribution. A turbulent kinetic energy k and an integral length scale L_t are required to set up the given energy spectrum. The monitoring of the resolved turbulent kinetic energy is performed as in the work of Janin *et al.* (2021) and the target resolved kinetic energy is here defined as

$$k_r^{\dagger} = k(1 - r_k) \tag{4}$$

In the present paper, an energy spectrum model suggested by Chaouat & Schiestel (2009) has been chosen as it is easy to integrate and thus leading to a straightforward expression for the kinetic energy ratio r_k.

$$r_k = \left[1 + \beta^{2/9}(\alpha_L L_t \kappa_{cut})^3\right]^{-2/9} \tag{5}$$

in which $\beta = (2/3C_k)^{2/9}$, $\alpha_L = 0.85$ and κ_{cut} is the cutoff wave number.

It mus be pointed out that the formulation of the target resolved kinetic energy is based on an assumption of conservation of the turbulent kinetic energy. Indeed, the proposed method aims to balance the resolved and subgrid turbulent kinetic energy budgets. Additional terms from the reconstruction procedure in Eq. 1 lead to a new production term in the resolved turbulent kinetic budget, as intented by the method. Note that the production term is not clipped, meaning it can exhibits negative values. This production term is added as a sink term to the subgrid kinetic energy transport equation. This allows to have a transfer of energy between the subgrid and the resolved part while formally keeping the total turbulent kinetic energy budget unchanged. This energy transfer must take place in under-resolved regions.

These regions are encountered when the observed turbulent kinetic energy ratio $r_k^o = k_{sgs}/k$ is greater than the kinetic energy ratio defined by Eq 5. Thanks to the control of the resolved turbulent kinetic energy, the forcing is only active in these regions. This makes the method self-adapting which prevents forcing in areas not of interest as coflow regions. This ensures that the solution does not deteriorate and saves computing times.

An attractive feature of the method is that the control of the resolved turbulent kinetic energy is done by a selective forcing. This selective forcing could either operates at low or high wavenumbers. For homogeneous isotropic turbulence, forcing at low wavenumbers is preferred as forcing at high wavenumbers alters the inertial zone of energy spectrum. In the case of turbulent shear flows the question arises. In their work, Haering (2022) argued for a forcing at high wavenumbers. That way large scales that may be present or the mean velocity flows are not disturbed by the forcing. Although we support this approach, preliminary results are not satisfactory. Therefore, the selective forcing at low wavenumbers is used in this work.

NUMERICAL SET UP

The proposed method is applied to a planar jet at a $Re = 10000$ which is based on the nozzle width $d_j = 0.05m$. Simulations are performed with the E-DES model and a mesh containing 7.510^5 grid points. The domain size is $[0;L_x] \times [0;Ly] \times [0;L_z]$ with $L_x = 40d_j$, $L_y = 40d_j$ and $L_z = 6.4d_j$, doubling the streamwise and normalwise dimensions compared to Engelmann *et al.* (2021). The fluid considered is air with constant physical properties, $\rho = 1.2kg.m^{-3}$ and $\mu = 1.810^{-5}kg.m^{-1}.s^{-1}$. Periodic conditions are used in the z-spanwise direction. An outlet-like condition that allows a control of the kinetic energy is imposed at the outlet that corresponds to the right, top and bottom boundaries as illustrated on Fig. 1. At the inlet, an hyperbolic tangent profile is specified for the mean axial velocity U_j as in Le Ribault *et al.* (1999), with a coflow $U_{co}/U_j = 9\%$. No fluctuations are superimposed on the mean velocity profile in boundary conditions. In order to assess the overall effect of the reconstruction procedure, the RANS mode is enforced over a $6d_j$ long area (*i.e.* $r_k = 1$) downstream the nozzle while this ratio keeps its original formulation Eq. 5 downstream the black dashed line reported in Fig. 1.

Simulation results are obtained using the in-house CALIF^{3}S-P^{2}REMICS software. Time discretization is carried out by using a fractional step algorithm that consists in a pressure correction method. Space discretization is performed by using a staggered finite volume scheme for which scalar unknowns are located at cell centers while the velocity is located at cell faces. The numerical scheme is discretely kinetic energy conserving (Boyer *et al.* (2014)) and corresponds to a centered second-order spatial discretization of both convective and diffusive fluxes together with the semi-implicit Crank-Nicolson time scheme. The time step is fixed according to the CFL based on the inlet mean velocity and the mesh size to be 0.5. The final time of the simulation is 40 flow time units and a restart is performed at 10 flow time units. The flow time units is defined as in Stanley (2002): $T_t = 2L_x/\left(U_j + U_{co}\right)$.

Results are compared with a simulation with turbulent inlet boundary condition, refereed here as turbulent BC. Turbulent fluctuations are generated with the RFM method and added to the mean velocity profile at the inlet. A RANS computation is also performed with a classical k-ε turbulence model. For both above mentioned computations, the same numerical parameters and physical properties are used. The different inlet parameters are summarized in Table 1.

Table 1: Summary table of inlet parameters for the zonal simulation with forcing and the simulation with turbulent Boundary Condition (BC)

Inlet parameters	Forcing/RANS	Turbulent BC
Re	10^4	10^4
Length scale	$0.4d_j$	$0.4d_j$
Turbulent intensity	10%	10%
Synthetic method	-	RFM
Mean profiles	hyperbolic tangent	hyperbolic tangent
Turbulent kinetic energy	peaks in the shear layer	peaks in the shear layer
Turbulent kinetic energy ratio	1	0.3

RESULTS

In this section, we investigate the influence of the reconstruction method by focusing on several quantities of interest such as the mean and root mean square values of the velocity in the self-similar region as well as the axial evolution of the turbulent kinetic energy. The slope coefficients of the jet half-width evolution and the decrease of the axial mean velocity excess are also compared to the results from the literature. Since we are emulating a zonal hybrid RANS/LES model, there is a transition area in between the two domains. Hence, it is interesting to assess these slope coefficients both in the transition area and further downstream.

This transition zone is highlighted on the snapshot of the instantaneous velocity displayed in Fig. 1. The black dashed line delimits the upstream RANS domain ($r_k = 1$) and the zone where the E-DES model behaves self-adapting. As expected, no velocity fluctuations are observed upstream of the black dashed line while the forcing enables the generation of fluctuations downstream. The transition area takes place just after the RANS domain. In this transition region, it appears that the jet-half width evolution is reduced over a distance of at least 7 diameters.

In order to discuss quantitative results, the effect of the proposed approach on statistical quantities needs to be assessed. All statistical quantities presented after are averaged over $30T_t$. First of all, the results in the self similar region are presented in Fig. 3 and are compared to results from the literature. Results are also compared to the simulation using turbulent boundary condition.

Radial profiles are presented for seven different axial locations between $x = 11d_j$ and $x = 28d_j$. Fig. 2a shows the normalwise evolution of the mean axial velocity for different axial positions. Results are in good agreement with results from the literature and the turbulent BC simulation. Mean velocity profiles collapse to a self-similar state except the profile at $x = 11d_j$ meaning that the self-similarity region is not yet reached at this location.

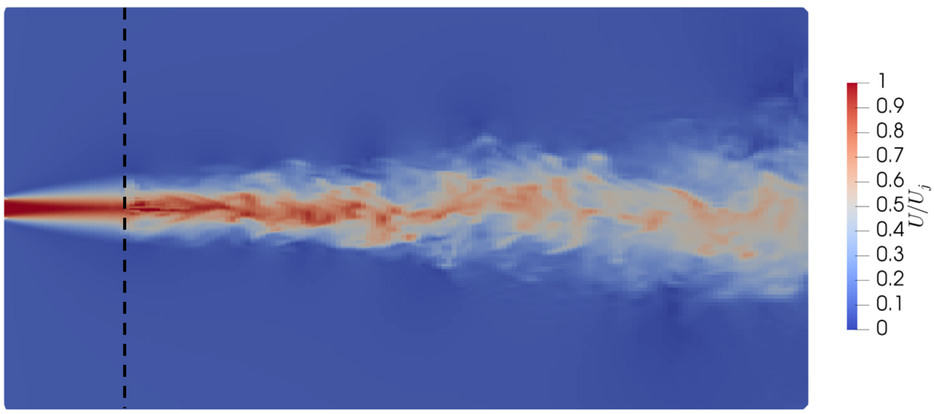

Figure 1: Instantaneous snapshot of the velocity magnitude. The black dashed line delimits the upstream RANS domain from the downstream E-DES domain at the axial position $x = 6d_j$.

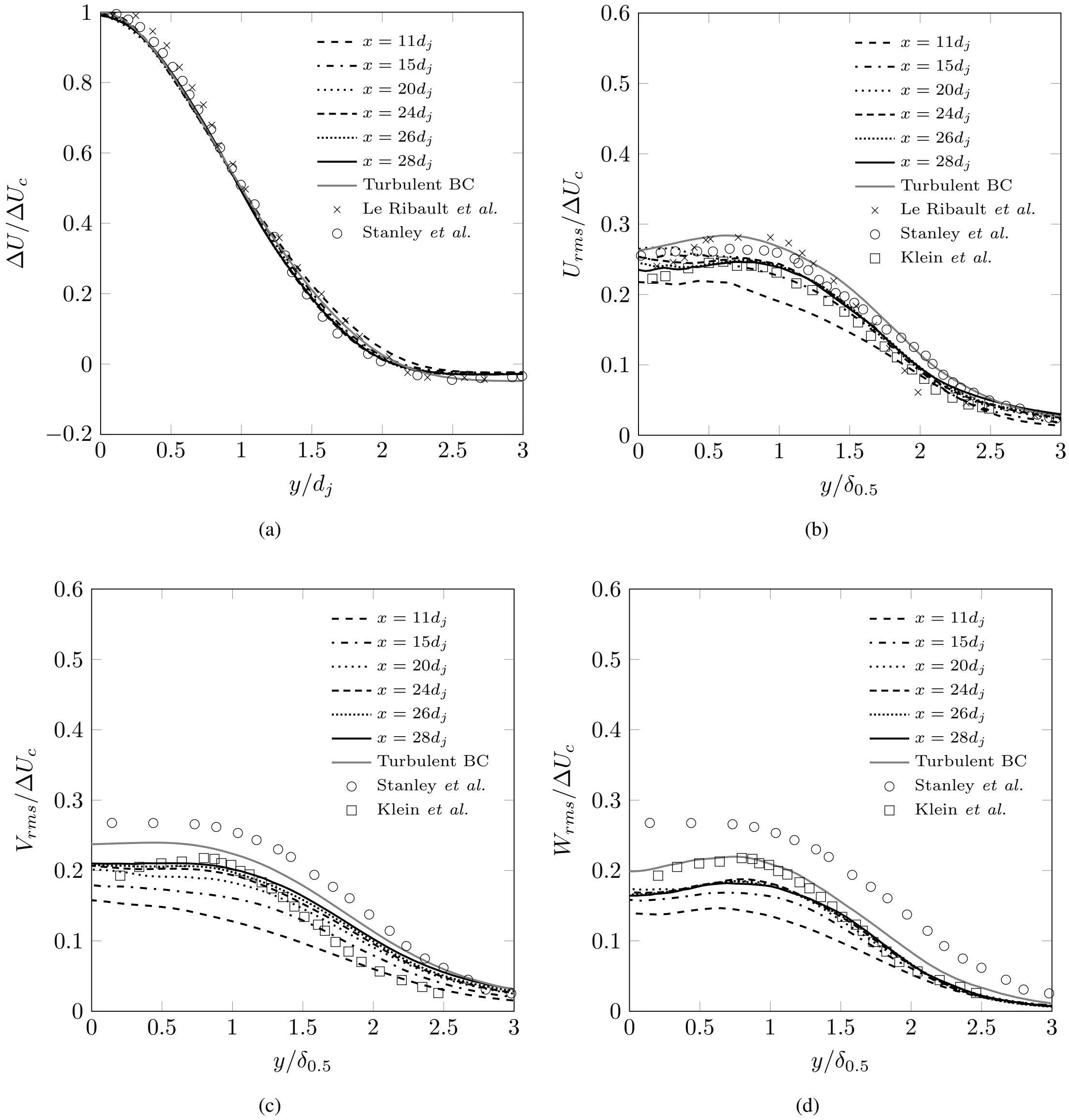

Figure 2: Radial profiles in the self-similarity region. (a) Mean streamwise velocity, (b) Streamwise velocity fluctuations U_{rms}, (c) Normalwise velocity fluctuations V_{rms} and (d) Spanwise velocity fluctuations W_{rms}.

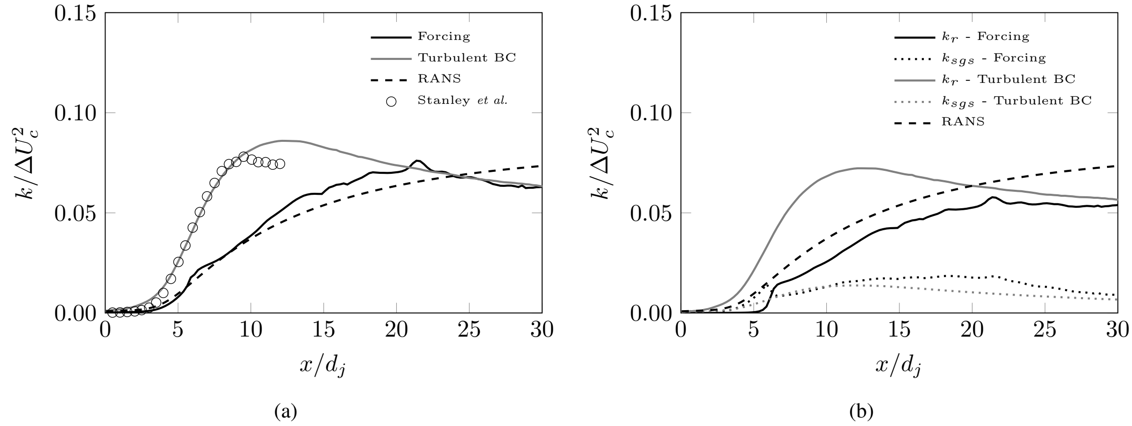

Figure 3: (a) Axial evolution of the turbulent kinetic energy. Comparison between the forcing method, the turbulent BC simulation and the DNS results from Stanley (2002), (b) Axial evolution of the resolved and subgrid turbulent kinetic energy. Comparison between the forcing method, the turbulent BC simulation and the RANS turbulent kinetic energy.

Radial profiles of the streamwise velocity fluctuations shown in Fig. 2b exhibit the same trends, namely that the jet becomes self-similar at $x = 11d_j$. Profiles are not in agreement near the center line before merging from $y/\delta_{0.5} = 1$. Nevertheless, there seems to be a convergence between profiles at position $x = 26d_j$ and $x = 28d_j$. The results are underestimated, in comparison with the turbulent BC simulation but are in good agreement with DNS and LES data from the literature.

Fig. 2c and Fig. 2d represent respectively radial profiles of the normalwise and spanwise velocity fluctuations. From these two figures, it appears that the profiles collapse to a self-similar behavior from $x = 20d_j$. Profiles are again underestimated compared to the turbulent BC simulation and the DNS results. For the V_{rms} radial profiles of the simulation with turbulent boundary condition, the self-similarity region is reached at $20d_j$ (not shown here). The same value seems to be obtained for the zonal simulation.

The underestimation of the fluctuating velocity profiles is reflected in Fig. 3a which represents the axial evolution of the turbulent kinetic energy. Regarding the RANS computation, the peak of turbulent kinetic energy is clearly underestimated compare to the DNS results. The turbulent kinetic energy reaches the same level as the simulation with turbulent boundary condition near $x = 20d_j$. Thanks to the forcing the turbulent kinetic energy does not decrease downstream the RANS domain and agrees well with the RANS results.

Fig. 3b shows the axial evolution of the energy distribution between the resolved and subgrid part also compared to the RANS turbulent kinetic energy. As expected, the increase of the resolved part starts from $x = 6d_j$ for the zonal configuration. At the same location, the subgrid kinetic energy decays due to the sharp decrease of the kinetic energy ratio and the production term which is subtracted from the right hand side of the subgrid turbulent kinetic transport equation.

It must be noticed that the reconstruction method has no influence on the ability of mean and fluctuating velocity profiles to converge towards self-similarity. The turbulent kinetic energy at the jet center line, is underestimated. However this is mainly due to the fact that the upstream RANS statistics are not reliable.

In order to estimate the impact of the proposed approach on the jet half width evolution and the mean excess velocity decay, the coefficients of the linear relationship that holds in the self-similar region are compared (Stanley (2002)):

$$\frac{\delta_{0.5}}{d_j} = K_1 \left(\frac{x}{d_j} + K_2 \right) \quad (6)$$

$$\left(\frac{\Delta U_j}{\Delta U_c} \right)^2 = C_1 \left(\frac{x}{d_j} + C_2 \right) \quad (7)$$

in which, ΔU_j and ΔU_c represent respectively the inlet velocity excess and the local center line velocity excess. These coefficients are calculated over a distance of $6d_j$, from $10d_j$ to $16d_j$. For the forcing case, coefficients are additionally computed for the region $[20d_j; 26d_j]$ since the first region is closed to the transition area. The resulting values are reported in Table 2. In the first region, the slope of the jet half width evolution is low compared to simulation with turbulent boundary condition. In the second region, the slope approaches the RANS results but is still underestimated compared to the DNS results. The same conclusions are made for the slope of the axial evolution of the velocity excess. This decay observed on the results is still under investigation and is part of the limitations of the method. The quality of the synthetic fluctuations introduced in the domain might play an important role in recovering more accurate slopes.

Table 2: Summary of the resulting coefficients K1, K2, C1 and C2 for the region $[6d_j; 12d_j]$.

Simulations	K1	K2	C1	C2
Forcing $[10d_j; 16d_j]$	0.062	3.44	0.138	1.19
Forcing $[20d_j; 26d_j]$	0.069	1.83	0.155	-0.61
Turbulent BC	0.096	1.47	0.196	0.066
RANS	0.082	2.16	0.168	0.273
Stanley (2002)	0.092	2.63	0.201	1.23

Conclusion

The reconstruction procedure proposed in Janin *et al.* (2021) is applied to the case of a planar jet at $Re = 10000$. The approach is extended to take into account the non-homogeneity of the flow. This results in an extra forcing term related to the reconstruction of the convective term in the filtered Navier-Stokes equations. The overall approach is assessed on a given configuration which roughly consists in a zonal hybrid RANS/LES method. By design, the forcing is only active downstream the RANS domain and target properties such as the resolved turbulent kinetic energy are provided by a prescribed turbulent kinetic energy ratio.

The reconstruction method allows to recover the self-similarity region. However, a transition zone appears in which mean quantities such as slopes of both the jet half width evolution and the mean velocity excess decay are significantly decreased. An improvement in the quality of the synthetic fluctuations might help to fine-tune the previously computed slopes. Typically, poor estimation of turbulent quantities in the upstream RANS domain contributes here to a large transition towards a fully developed self-similar behavior.

The expected benefits of the proposed approach should be at first a reduction of the computational cost by using a CFL constraint built far from the slot where the characteristic mean velocity has decreased drastically. A substantial benefit is also expected for buoyant jets as LES usually exhibits superior predictive capabilities far from the nozzle in the dominated buoyant region while RANS predictions remain accurate near the nozzle in the dominated inertia region.

REFERENCES

Bentaib, A., Meynet, N. & Bleyer, A. 2015 Overview on hydrogen risk research and development activities: methodology and open issues. *Nuclear Engineering and Technology* **47** (1), 26–32.

Boyer, F., Dardalhon, F., Lapuerta, C. & Latché, J.-C. 2014 Stability of a crank-nicolson pressure correction scheme based on staggered discretizations. *International Journal for Numerical Methods in Fluids* **74**, 34–58.

Chaouat, B. & Schiestel, R. 2009 Progress in subgrid-scale transport modelling for continuous hybrid non-zonal rans/les simulations. *Int. J. Heat Fluid Flow* **30**, 602–616.

Engelmann, L., Klein, M. & Kempf, A.M. 2021 A-posteriori les assessment of subgrid-scale closures for bounded passive scalars. *Comput. Fluids* **218**, 104840.

Friess, C., Manceau, R. & Gatski, T.B. 2015 Toward an equivalence criterion for hybrid rans/les methods. *Comput. Fluids* **122**, 233–246.

Fung, J.C.H., Hunt, J.C.R., Malik, N.A. & Perkins, R.J. 1992 Kinematic simulation of homogeneous turbulence by unsteady random fourier modes. *J. Fluid Mech* **236**, 281–318.

Haering, S. W., Oliver T. A. Moser R. D. 2022 Active model split hybrid rans/les. *Physical review fluids* **7**, 014603.

Janin, J., Duval, F., Friess, C. & Sagaut, P. 2021 A new linear forcing method for isotropic turbulence with controlled integral length scale. *Phys. Fluids* **33**, 045127.

Klein, M., Sadiki A. Janicka J. 2003 Investigation of the influence of the reynolds number on a plane jet using direct numerical simulation. *Heat and Fluid Flow* **24**, 785–794.

Kraichnan, R.H. 1970 Diffusion by a random velocity field. *Phys. Fluids* **13**, 22.

Le Ribault, C., Sarkar, S. & Stanley, S.A. 1999 A-posteriori les assessment of subgrid-scale closures for bounded passive scalars. *Phys. Fluids* **11**, 3069.

Lundgren, T.S. 2003 Linearly forced isotropic turbulence. *Annual Research Brief (CTR, Standford)* pp. 461–473.

de Laage de Meux, B., Audebert, B., Manceau, R. & Perrin, R. 2015 Anisotropic linear forcing for synthetic turbulence generation in large eddy simulation and hybrid RANS/LES modeling. *Phys. Fluids* **27**, 035115.

P^{2}REMICS 2021 Collaborative website - https://gforge.irsn.fr/gf/project/p2remics/.

Pamier, M, Weiss, P. E., Garnier, E, Deck, S & Sagaut, P 2009 Generation of synthetic turbulent inflow data for large eddy simulation of spatially evolving wall-bounded flows. *Phys. Fluids* **21**, 045103.

Schmidt, S. & Breuer, M. 2017 Source term based synthetic turbulence inflow generator for eddy-resolving predictions of an airfoil flow including a laminar speration bubble. *Comput. Fluids* **146**, 1–22.

Stanley, S. A., Sarkar S. Mellado J.P 2002 A study of the flow-field evolution and mixing in a planar turbulent jet using direct numerical simulation. *J. Fluid Mech* **450**, 377–407.

Taveau, J. 2011 Explosion hazards related to hydrogen releases in nuclear facilities. *Journal of loss prevention in the process industries* **24** (1), 8–18.

Zhang, J. 2021 Significance of generating synthetic turbulence for zonal detached eddy simulation of shallow water flows. *Ocean Engineering* **237**, 109418.